The structure of fluorinated indazoles: the effect of the replacement of a H by a F atom on the supramolecular structure of NH-indazoles†

Johannes Teichert,[a] Pascal Oulié,[a] Kane Jacob,[a] Laure Vendier,[a] Michel Etienne,*[a] Rosa M. Claramunt,*[b] Concepción López,[b] Carlos Pérez Medina,[b] Ibon Alkorta[c] and José Elguero[c]

The structures of three NH-indazoles (3-methyl, 3-trifluoromethyl and 3-trifluoromethyl-4,5,6,7-tetrafluoroindazoles) have been determined by X-ray crystallography. These three compounds, together with 3-methyl-4,5,6,7-tetrafluoroindazole, whose X-ray structure could not be determined, have been studied using multinuclear magnetic resonance spectroscopy, including solid-state CPMAS. They all are 1H-tautomers. In the crystal, 3-methyl-1H-indazole forms hydrogen bonded dimers, whereas 3-trifluoromethyl-1H-indazole and 3-trifluoromethyl-4,5,6,7-tetrafluoro-1H-indazole crystallize as catemers. These catemers are chiral space group $P3_2$. They are the first examples of indazoles crystallizing in the form of helices of three-fold screw axis. Attempts at rationalizing this behavior on the basis of supramolecular interactions (hydrogen bonds and aromatic interactions) and GIAO calculations are discussed.

Introduction

Indazoles or benzo[c]pyrazoles are much less known than pyrazoles although some important compounds contain an indazole skeleton,[1] amongst them Granisetron 1[1a] (and the related drug, Indisetron),[2] and especially the new inhibitors of neuronal nitric oxide synthase (NOS), 2–4 (Scheme 1).[3] On the other hand, the best known trifluoromethyl substituted drug is Celecoxib 5 (Scheme 1).[1b] Besides, in the last decade, molecular interactions in a variety of organic compounds involving fluorine substituents have gained interest in life sciences and materials.[4–6]

In view of these properties and those related to the use of indazoles as ligands (or as part of ligands) in coordination chemistry,[7] we decided to investigate the fluorinated derivatives of 3-methyl-1H-indazole (6).

First, a summary of the structural knowledge of NH-indazoles is useful. All indazoles are 1H-tautomers and only with a combination of several C-substituents, which does not apply in the present study, do the 2H-tautomers become predominant.[8–10] Concerning NMR spectroscopy, the three nuclei present in indazoles have been studied: [1]H, ^{13}C and [15]N.[11–13] The crystal structures of several NH-indazoles have been determined and the literature on this topic reviewed
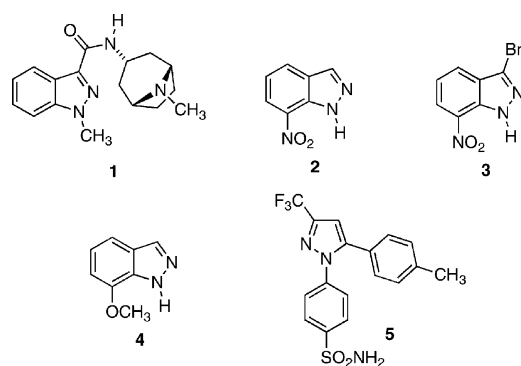
Scheme 1   Indazoles and a 3-trifluoromethylpyrazole of biological relevance.

recently.[14] To date, N–H···N hydrogen bonds are always present in crystals of indazoles. Although no structural correlation with their substitution pattern has so far been found, indazoles crystallize in the form of dimers, trimers or catemers with two-fold screw axes. In this paper, we report the synthesis and the structural characterization by multinuclear NMR spectroscopy and X-ray crystallography of a family of variously fluorinated 3-methyl-1H-indazoles, including 3-methyl-1H-indazole (6) itself. For the first time, a remarkable supramolecular arrangement of helical catemers with three-fold screw axes is observed for the fluorinated 3-methylindazoles. Attempts at rationalizing these structures with the aid of GIAO calculations are discussed.

Results

The present paper focuses on the four related 1H-indazoles 6–9 depicted in Scheme 2.

[a] *Laboratoire de Chimie de Coordination du CNRS, UPR 8241 liée par conventions à l'Université Paul Sabatier et à l'Institut Polytechnique de Toulouse, 205 Route de Narbonne, F-31077 Toulouse Cedex 4, France. E-mail: etienne@lcc-toulouse.fr*
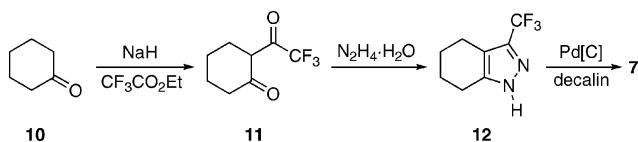[b] *Departamento de Química Orgánica y Bio-Orgánica, Facultad de Ciencias, UNED, Senda del Rey 9, E-28040 Madrid, Spain. E-mail: rclaramunt@ccia.uned.es*
[c] *Instituto de Química Médica, CSIC, Juan de la Cierva 3, E-28006 Madrid, Spain*
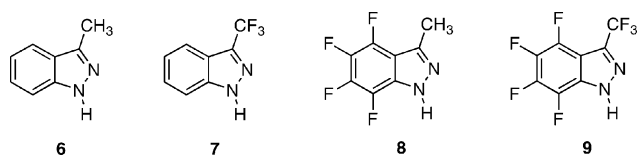
Scheme 2 The four studied indazoles.

Scheme 3 Preparation procedure for indazole 7 (overall yield 8%).

Scheme 4 Preparation procedure for indazole 9 (overall yield 32%).

Synthesis
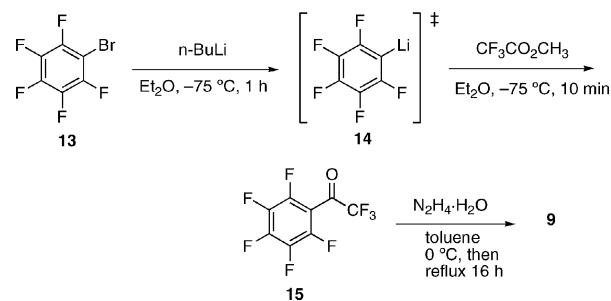
3-Methyl-1H-indazole (6),[15,16] 3-trifluoromethyl-1H-indazole (7),[17,18] and 3-methyl-4,5,6,7-tetrafluoro-1H-indazole (8)[19] are known compounds whereas 3-trifluoromethyl-4,5,6,7-tetra-fluoro-1H-indazole (9) is new. In this study, we have prepared 7 via another approach, the aromatization of the corresponding tetrahydroindazole. Following the procedure described in Scheme 3, 7 was obtained from cyclohexanone 10 in 8% overall yield.

Compound 9 was prepared using the procedure depicted in Scheme 4, which is similar to the method[19] Glaser et al. used to make 8 but using octafluoro- instead of pentafluoroaceto-phenone.

Pentafluorobromobenzene 13 was treated with n-butyllithium to yield the reactive intermediate pentafluorobenzenelithium 14. This was transformed directly to octafluoroacetophenone 15 by addition of methyl trifluoroacetate. In fact, this reaction proved to be crucial for the overall yield, since compound 15 is highly activated at the electrophilic carbonyl carbon and the longer the reaction proceeded, the higher the percentage of unwanted by-products. Attempts at improving the yield by using trifluoro-acetic anhydride failed. The cyclization was realized by adding hydrazine hydrate to the reaction mixture of 15 without puri-fication and heating to reflux in toluene to yield the desired 3-trifluoromethyl-4,5,6,7-tetrafluoro-1H-indazole 9. The yield for the three steps was 32%. From pure commercial octafluoroa-cetophenone, the yield is 79%.

Crystal structures

The crystal structures of three of the compounds, namely 6, 7 and 9, have been obtained.‡ Strikingly, 7, 8 and 9 crystallize in the form of long, hair-like needles and, as reported pre-viously,[19] crystals of 8 suitable for X-ray diffraction could not be obtained. The major difference between the 3-methy-lindazole 6 and the fluoro-containing 3-trifluoromethylinda-zoles 7 and 9 (the perfluoro version of 6) resides in the arrangement of the molecules in the crystal. Indazole 6 crystal-

‡ CCDC 615981 (6), CCDC 615982 (7), and CCDC 615983 (9). For crystallographic data in CIF or other electronic format see DOI: 10.1039/b617988f

lizes in the monoclinic system, space group $P2_1/n$. Fig. 1 shows a molecule of 6.

As can be seen in Fig. 2, 6 forms dimers connected by two N–H···N hydrogen bonds: N(1)–N(2) = 1.3693(15), N(1)···N(2)′ = 2.99, N(1)–H(1) = 0.89 Å; N(1)–H(1)–N(2)′ = 142°. The two units of each dimer are related by an inversion center. They are parallel to each other but not coplanar, with a distance of 0.54 Å between the planes. Contacts between dimeric units indicate no significant aro-matic interactions (angles between planes, 59 and 121°; dis-tances between centroids of benzo rings, 4.97 and 5.72 Å, respectively; distances between the centroid of a benzo ring and next plane, 4.75 Å, offset 1.46 and 3.20 Å, respectively) (for the definition of aromatic interactions, see ref. 20). There are close contacts between a CH$_3$ group of one indazole and a benzo group of a single neighboring indazole (distance be-tween C and centroid/plane, 3.81/3.75 Å), suggesting possible but weak C–H···π interactions, although no hydrogen from the methyl group points directly at the benzene ring (distance between the closest methyl H and centroid/plane, 3.17/3.01 Å; C–H-centroid/plane angle 125/59°).[21] This situation is differ-ent from that of the CF$_3$ group in 7 and 9 as described below.

By contrast, 7 and 9 both crystallize in a chiral space group. Since there were no significant anomalous scatterers, it was not possible to decide between space groups $P3_1$ and $P3_2$. $P3_2$ was arbitrarily chosen. These indazoles are two new remarkable examples of spontaneous chiral resolution in which a non-chiral molecule crystallizes in a chiral space group. Only one type of helix, either M or P, is found in the crystal, although it is not possible to determine which one (see experimental section). The molecular structures of 7 and 9 are shown in Fig. 3 and Fig. 4, respectively.

Molecules of 7 (Fig. 5) and 9 (Fig. 6) are arranged in helical chains (catemers) whose three-fold axes are oriented along the c axis. Molecules in the helices are connected by an N–H···N hydrogen bond network (for 7, N(1)···N(2)′ = 2.89, N(1)–H(1) = 0.86 Å, N(1)–H(1)–N(2)′ = 177°; for 9, N(1)···N(2)′ = 2.90, N(1)–H(1) = 0.86 Å, N(1)–H(1)–N(2)′ = 176°) but also, most probably, by aromatic interactions that depend on the fluorine content of the benzo rings. Indeed, the planes of two consecutive molecules along the chains of 7 and 9 are tilted 57 and 73°, respectively. The planes of equivalent molecules of 7 and 9 related by the full three-fold symmetry along the chains are separated by 3.63 and 3.58 Å, respec-tively. Pertinent parameters defining the interactions between these molecules are gathered in Table 1. Views perpendicular
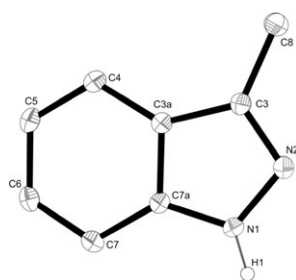
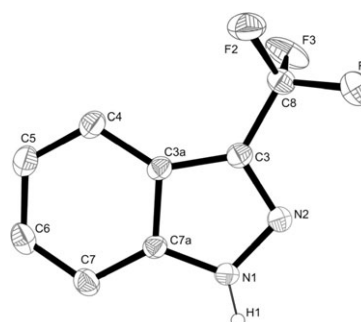**Fig. 1** Molecular structure of **6**.

Fig. 3 Molecular structure of **7**.

to the plane of the stacking molecules are shown in Fig. 7 (for **7**) and Fig. 8 (for **9**).

According to prevailing analyses,[5,6,20] these stackings result from attractive interactions. Recall that in fluoroaromatics the charge distribution is inverted as compared to that in perprotio aromatics, so that the center of the fluorinated benzo ring carries a formal positive charge with negative fluorines outside.[22] The offset stacking as described in Table 1 is a manifestation of these effects. There are then several short intermolecular F···C contacts. For **7**, F(1) from a trifluoromethyl group of one molecule and F(3) of the stacking molecule along the chain are separated by 2.89 Å, which is less than the sum of the van der Waals radii (2.94 Å). However with C–F···F angles of *ca.* 113°, these close contacts are attributed to packing effects.[6] There are no such intermolecular *intrachain* CF₃···CF₃ close contacts for **9**. Similarly, CF₃···F–C(aromatic) contacts are, most likely, not significant because of the angles being very obtuse. Fig. 5–8 show the relative orientations of the CF₃ groups with respect to either the benzo or pyrazolyl rings of stacking molecules. The conformations of the CF₃ groups do not seem influenced by these close contacts since they are very similar in both compounds (torsion angles F(1)–C(8)–C(3)–N(2) are −26° and −20° for **7** and **9**, respectively). For indazole **9** *interchain* interactions between aromatic C–F bonds may well be present. As depicted in Fig. 9, there are short aromatic C–F···F–C contacts (2.82 Å) with C–F···F angles of 98° and 148° that suggest possible attractive interactions.[6]
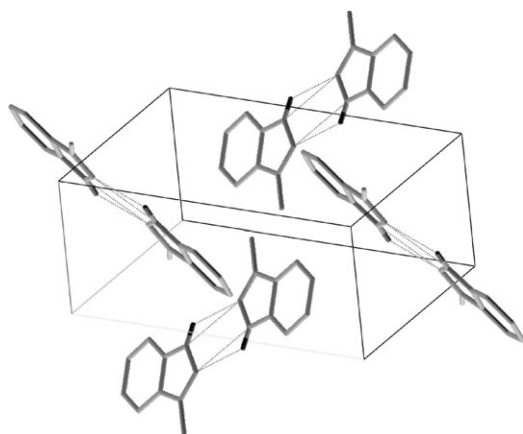
NMR spectroscopy

The chemical shifts and coupling constants of compounds **6–9** are reported in Table 2 (¹H in CDCl₃ solution), Table 3 (¹³C in CDCl₃ solution and in solid state), Table 4 (¹⁵N in DMSO-d₆ or CDCl₃ solution and in solid state) and Table 5 (¹⁹F in CDCl₃ solution and in solid state). For the first three nuclei, the assignments are based on standard 2D experiments and on comparison with literature data, which are extensive for these nuclei.[11–13] There has been no previous study on ¹⁹F NMR of indazoles. Obviously, the CF₃ signals are easy to identify, having chemical shifts very similar to those of trifluoromethyl-pyrazoles.[23]

To assign the fluorine atoms at positions 4, 5, 6 and 7 for compounds **8** and **9**, we have used $^1J_{^{13}C-^{19}F}$ coupling constants. In Table 3, these couplings are: C-4 (252.4 and 256.4 Hz), C-5 (245.3 and 250.1 Hz), C-6 (251.2 and 255.0 Hz) and C-7 (249.9 and 251.2 Hz), respectively. These couplings, although obtained through a first order analysis, are strictly proportional, eqn (1), reflecting the effect of replacing a CH₃ by a CF₃ group.

$$^1J(\mathbf{9}) = (33 \pm 10) + (0.88 \pm 0.04) \, ^1J(\mathbf{8}),$$
$$n = 4, r^2 = 0.996 \tag{1}$$

The same coupling constants (±0.2 Hz) were obtained from the ¹³C satellites in the ¹⁹F NMR spectra, securing the interpretation.
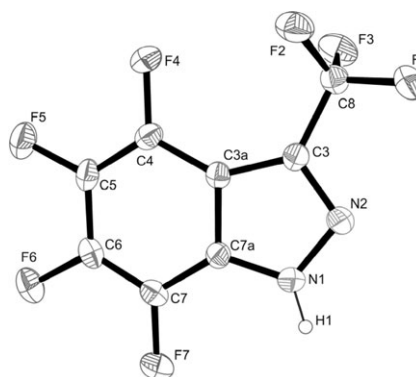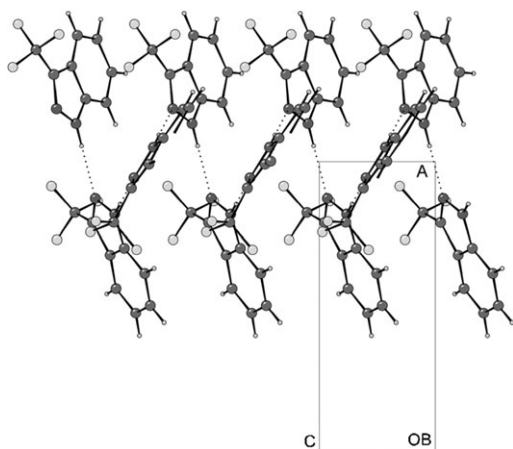

Fig. 2 Molecular packing of **6**.

Fig. 4 Molecular structure of **9**.

Fig. 5 Molecular packing of **7**.

Table 1 Metric parameters between two equivalent parallel molecules of **7** and **9** along the chains

Compound	Ctd–ctd/Å[a]	Ctd–plane/Å[b]	Offset/Å
7	4.35	3.63	3.91
9	4.95	3.58	3.42

[a] Distance between equivalent centroids. [b] Distance between a centroid and the interacting plane.

Fig. 7 Perpendicular view to the plane of stacking for **7**.

Discussion

Structural crystallography

The three compounds described herein are all 3-substituted 1*H*-indazoles. The characteristic C7a–N1–N2 and N1–N2–C3 angles are, respectively, 111.8 and 106.5° (**6**), 112.2 and 105.3° (**7**), and 111.6 and 105.9° (**9**). These values are to be compared with the calculated geometries at the B3LYP/6-311++G** level: the average values for the four 1*H*-indazoles are 112.4 and 106.5°, respectively, whereas for the four 2*H*-indazoles, they are 103.5 and 115.5°, respectively. Similarly, characteristically long C3a–C3 bonds (1.4264(18), 1.413(6) and 1.405(6) Å for **6**, **7** and **9**, respectively) and short C3–N2 bonds (1.3203(16), 1.329(6) and 1.334(5) Å for **6**, **7** and **9**, respectively) are observed.[9] The main difference between them is the presence of a CF$_3$ group in **7** and **9** which crystallize as helices as opposed to a CH$_3$ group in **6** which crystallizes as a dimer. As a strong electron-withdrawing substituent, a trifluoromethyl group strongly influences the acidity of the NH proton
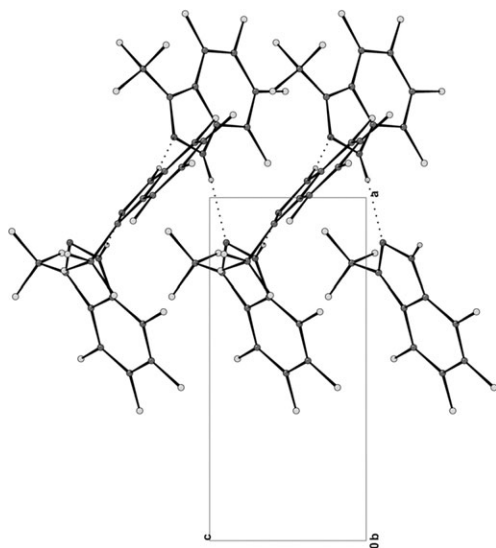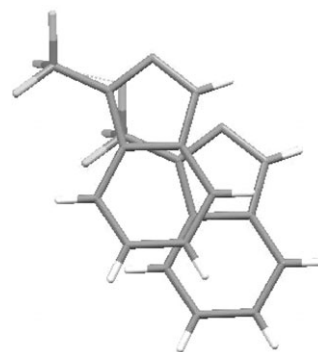
(and consequently the strength of N–H···N hydrogen bonds) and the possible aromatic interactions between the indazole rings. Electron-withdrawing substituents enhance attractive π-interactions.[20] Indeed, whatever the H/F substitution pattern of the benzo rings in **7** and **9**, the aromatic interactions are always attractive between two equivalent molecules along the chains. The different topology of the two chains can be accounted for by these substitutions (Fig. 7 and 8). The markedly different angles between planes of successive molecules along the chains (57 and 73°, for **7** and **9**, respectively) are most probably the result of such optimized interactions. Although it is not supported by X-ray diffraction, crystal habit (long needle-like crystals) and NMR data supported by calculations (see below) strongly suggest that **8** crystallizes as a catemer as well (with no indication of its eventual pitch). *Overall, the helical arrangement would be attributable to either or both the benzo ring or the 3-methyl group being perfluorinated, i.e. to the introduction of either or both of these strongly electron-withdrawing groups.* Different substitution patterns then influence competing forces (hydrogen bonds, aromatic interactions in a broad sense, and steric interactions), yielding
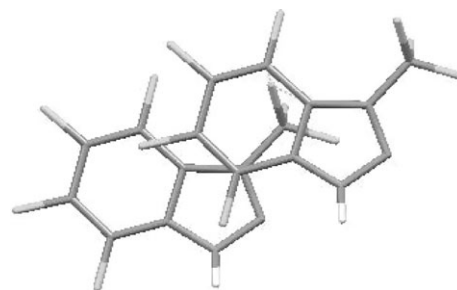

Fig. 6 Molecular packing of **9**.

Fig. 8 Perpendicular view to the plane of stacking for **9**.
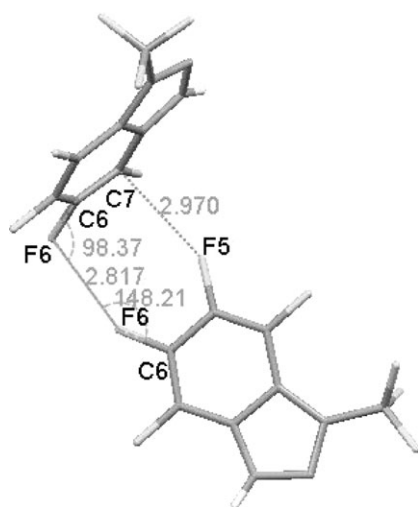
Fig. 9 CF–FC contacts and CFF angles for **9**.

Table 2 ^{1}H NMR chemical shifts (ppm) and ^{1}H–^{1}H coupling constants (Hz) of indazoles in CDCl$_3$

Inda-zole	N(1)–H	R-3	H-4	H-5	H-6	H-7
6	10.60 (vbr)	CH$_3$: 2.66 (br)	7.70 (dd)	7.15 (ddd)	7.38 (ddd)	7.45 (dd)
			$^3J_{45} = 8.1$	$^3J_{56} = 7.5$	$^3J_{67} = 8.2$	
			$^4J_{46} = 1.1$	$^4J_{57} = 1.0$		
7	11.14 (vbr)	CF$_3$: —	7.88 (dd)	7.33 (ddd)	7.50 (ddd)	7.59 (dd)
			$^3J_{45} = 8.3$	$^3J_{56} = 7.6$	$^3J_{67} = 7.8$	
			$^4J_{46} = 1.0$	$^4J_{57} = 0.9$		
8	11.60 (br)	CH$_3$: 2.57 (s)	—	—	—	—
9	11.94 (br)	CF$_3$: —	—	—	—	—

vbr: very broad signal; s: singlet; d: doublet.

different helical parameters. This situation is akin to that of some pyrazole derivatives like 3,5-dimethyl-4-nitropyrazole which crystallizes as a helix of order 3, whereas 3,5-dimethyl-pyrazole crystallizes as a trimer.[24] In general, for NH-pyrazoles, the distance between the centroids of the five-membered rings is 4.1 Å on average for a helix of order 3, which corresponds to a pitch of 1.37 Å.[25] In the case of compounds **7** and **9**, these values become 4.64 Å (pitch 1.55 Å) and 4.95 Å (pitch 1.65 Å), respectively. This increase is consistent with indazoles being more bulky than pyrazoles.

Comparison with the structures of other indazoles is also interesting. As summarized in a recent article,[14] 1H-indazoles crystallize as N–H$\cdots$N arrangements, whose substructures are either in the form of dimers, trimers or catemers (we exclude 4-nitro-7-phenylsulfonylmethylindazole[26] which exhibits N–H$\cdots$O=N bonds). Before this work, no indazole was found in the form of helical chains with three-fold symmetry. 7-Nitroindazole[27] **2** and 5-nitro-3-thiomorpholinoindazole[28]

crystallize as dimers. Trimers are found for 7-methoxyindazole **4**,[3d] for two polymorphic forms of 3-phenylindazole,[30] for 3-phenyl-5-methylindazole[31] and for 3-methylcarboxyindazole.[32] The parent 1H-indazole,[33] 5-phenylindazole[29] and 7-methylindazole[14] crystallize as one-dimensional catemers (two-fold screw axes). Obviously the formation of dimers, including **6**, is not due to any specific substitution pattern. Selecting the 3-substituted indazoles, we see that a dimer (*i.e.* **6**), three trimers and two catemers with three-fold screw axes (*i.e.* **7** and **9**) exist. It is tempting to relate the supramolecular arrangements to the overall electronic properties of the substituents. As we go from the dimer to the trimers and eventually to the helices, the electron-withdrawing properties of the substituents strongly increase. Certainly, the effect is more complex, but as mentioned above, this drastically modifies the N–H$\cdots$N bond strength and the electron density at the aromatic rings. We tentatively suggest that aromatic interactions, albeit weak, would contribute by switching from a

Table 3 ^{13}C NMR chemical shifts (ppm) and ^{1}H–^{13}C or ^{19}F–^{13}C coupling constants (Hz) of indazoles in solution and in solid state

Indazole	Solvent	C-3	C-3a	C-4	C-5	C-6	C-7	C-7a	R-3
6	CDCl$_3$	143.2 (q) $^2J = 5.9$	122.7 (bs)	120.1 (ddd) $^1J = 160.0$ $^2J = 3.0$ $^3J = 7.8$	120.2 (ddd) $^1J = 160.0$ $^2J = 3.0$ $^3J = 7.8$	126.7 (ddd) $^1J = 158.2$ $^2J = 3.3$ $^3J = 8.0$	109.7 (dd) $^1J = 163.1$ $^3J = 7.9$	141.1 (dd) $^3J = 8.8$ $^3J = 8.8$	12.0 (q) $^1J = 127.5$
	CPMAS	144.5	123.6	121.2	121.2	127.9	111.5	140.8	10.5
7	CDCl$_3$	135.6 (q) $^2J = 38.3$	119.4 (bs)	119.8 (dd) $^1J = 169.4$ $^3J = 8.0$	123.1 (dd) $^1J = 162.7$ $^3J = 7.6$	128.2 (dd) $^1J = 162.8$ $^3J = 7.9$	110.7 (dd) $^1J = 166.1$ $^3J = 7.9$	141.0 (dd) $^3J = 8.6$ $^3J = 8.6$	122.0 (q) $^1J = 268.9$
	CPMAS	134.7	119.4	120.9	122.1	126.9	109.1	140.6	120 (vbr)
8	CDCl$_3$	142.9 (br)	109.6 (d) $^2J = 16.3$	139.7 (dm) $^1J = 252.4$	135.0 (ddd) $^1J = 245.3$ $^2J = 15.7$ $^2J = 15.7$	139.8 (dddd) $^1J = 251.2$ $^2J = 16.3$ $^2J = 16.3$ $^3J = 2.5$	132.5 (ddddd) $^1J = 249.9$ $^2J = 13.8$ $^3J = 5.0$ $^4J = 2.5$	127.8 (ddd) $^2J = 13.8$ $^3J = 8.8$ $^3J = 3.8$	13.1 (q) $^1J = 127.3$
	CPMAS	141.6	108.2	139 (vbr)	134 (vbr)	139 (vbr)	134 (vbr)	126.5	12.2
9	CDCl$_3$	136.0 (q) $^2J = 41.5$	106.9 (d) $^2J = 21.4$	138.2 (dddd) $^1J = 256.4$ $^2J = 12.6$ $^3J = 3.8$ $^4J = 3.8$	137.3 (ddd) $^1J = 250.1$ $^2J = 15.2$ $^2J = 15.2$	140.4 (ddd) $^1J = 255.0$ $^2J = 14.4$ $^2J = 14.4$	132.5 (ddddd) $^1J = 251.2$ $^2J = 13.2$ $^3J = 5.7$ $^4J = 2.5$	127.8 (ddd) $^2J = 13.8$ $^3J = 7.5$ $^3J = 3.8$	120.3 (q) $^1J = 269.2$
	CPMAS	136.2	106.3	139 (vbr)	139 (vbr)	139 (vbr)	133 (vbr)	128.1	120 (vbr)

This journal is © the Royal Society of Chemistry and the Centre National de la Recherche Scientifique 2007

Table 4 ^{15}N NMR chemical shifts (ppm) and ^{1}H–^{15}N coupling constants (Hz) of indazoles

Indazole	Solvent	N-1	N-2	^{1}JN1–H	^{2}JN2–H
6	DMSO-d$_6$	−202.3	−71.2	105^a	—
	CPMAS	−205.1	−80.6	—	—
7	CDCl$_3$^{b}	−197.2	−82.5	—	—
	CPMAS	−195.1	−85.2	—	—
8	CDCl$_3$	N. o.^{c}	−77.5	—	—
	CPMAS	−202.3	−82.3	—	—
9	CDCl$_3$^{b}	−205.0	−75.2	110^a	—
	CPMAS	−200.0	−81.9	—	—

^{a} HMQC. ^{b} T = 213 K. ^{c} N. o. = not observed.

repulsive situation (electron-rich 3-methylindazole) to an attractive one (electron-poor fluorinated indazoles).

Beyond the problem of the forces that dictate one arrangement or another, **7** and **9** are rare examples of achiral molecules that crystallize in chiral space groups. Molecules able to form hydrogen bonds often form supramolecular infinite helical chains. In the majority of cases, chiral helices pack together in enantiomeric pairs mimicking the formation of racemic compounds. Most cases of spontaneous resolutions involve chiral molecules (conglomerates).[34] There are few examples of achiral molecules that generate crystals of one handedness and still fewer that involve helices.[24,35,36]

NMR spectroscopy

Here, we verify that solution and solid state tautomers are the same for all indazoles. Also, solid state NMR spectroscopy is used to show that compound **8** does crystallize as a helix. The section includes the GIAO computed absolute shieldings σ calculated at the B3LYP/6-311 + +G**//B3LYP/6-311 + +G** level (see computational study below). Since the ^{19}F signals were assigned from the ^{13}C signals, it is important to show the consistency of the latter ones. The fluorine SCS (substituent chemical shifts) can be found in Scheme 5. Considering that the assignments for compounds **6** and **8** are straightforward, the consistency of the values indicates correct assignment.

From the experimental values of Tables 3, 4 and 5 and the absolute shieldings (not reported) calculated at the GIAO/

B3LYP/6-311 + +G**//B3LYP/6-311 + +G** level, the following regression lines can be obtained:

$$\delta^{13}C(\text{solution}) = (170.8 \pm 1.1) − (0.88 \pm 0.02)\,\sigma^{13}C,$$
$$n = 28,\ r^2 = 0.985 \qquad (2)$$

$$\delta^{13}C(\text{CPMAS}) = (170.0 \pm 1.5) − (0.86 \pm 0.03)\,\sigma^{13}C,$$
$$n = 28,\ r^2 = 0.97 \qquad (3)$$

$$\delta^{15}N(\text{solution}) = −(147.6 \pm 1.9) − (0.79 \pm 0.02)\,\sigma^{15}N,$$
$$n = 8,\ r^2 = 0.994 \qquad (4)$$

$$\delta^{15}N(\text{CPMAS}) = −(149.3 \pm 1.4) − (0.75 \pm 0.02)\,\sigma^{15}N,$$
$$n = 8,\ r^2 = 0.997 \qquad (5)$$

The similitude of the pairs of eqn (2)–(3) and (4)–(5) indicates that the structures of the indazoles are the same in solution and in the solid state. In particular, they are all 1*H*-tautomers. We have calculated the four 2*H*-tautomers and they lie about 20 kJ mol$^{−1}$ higher in energy.

For ^{19}F (Table 5), the equation is:

$$\delta^{19}F(\text{solution}) = (158.7 \pm 7.8) − (0.95 \pm 0.02)\,\sigma^{19}F,$$
$$n = 10,\ r^2 = 0.995 \qquad (6)$$

To check the validity of eqn (6), we calculated the absolute shieldings of the fluoroaromatic compounds reported in ref. 37 (24 chemical shifts, from fluorobenzene, −113.1 ppm, to 1,2,3,4-tetrafluoronaphthalene, −151.1 and −159.9 ppm). Analyzing the values of Table 5 and the fluoroaromatic derivatives together, eqn (7), fully similar to eqn (6), is obtained.

$$\delta^{19}F(\text{solution}) = (164.0 \pm 4.0) − (0.97 \pm 0.01)\,\sigma^{19}F,$$
$$n = 34,\ r^2 = 0.994 \qquad (7)$$

The intercepts are close to the values of TMS (^{13}C: 184.7 ppm), MeNO$_2$ (^{15}N: −154.4 ppm) and CFCl$_3$ (^{19}F: 153.7 ppm) calculated at the same level.[38]

Comparison of the *calculated* chemical shifts for the isolated molecule and for the molecule in the crystal can be used to determine intermolecular interactions.[39] Although protons are better, ^{13}C signals can be used.[38] Comparison of the *experimental* chemical shifts of indazoles **6–9** in solution (assumed to represent the isolated molecule) and in the solid state is provided in Table 6. ^{19}F chemical shifts have not been used since there is no data for **6**. The ^{13}C chemical shifts of the substituents at position 3 (CH$_3$/CF$_3$) are not very useful,

Table 5 ^{19}F NMR chemical shifts (ppm) and ^{19}F–^{19}F coupling constants (Hz) of indazoles

Indazole	Solvent	F-4	F-5	F-6	F-7	3-CF$_3$
7	CDCl$_3$	—	—	—	—	−61.3 (s)
	CPMAS	—	—	—	—	−57.8
8	CDCl$_3$	−149.1 (dd)	−167.0 (td)	−157.0 (ddd)	−159.5 (ddd)	—
		J_{F5} = 19.0	$^3J_{F4}$ = 19.0	$^3J_{F5}$ = 19.0	$^3J_{F6}$ = 19.0	
		J_{F7} = 19.0	$^3J_{F6}$ = 19.0	$^3J_{F7}$ = 19.0	$^4J_{F5}$ = 3.0	
			$^4J_{F7}$ = 3.0			
	CPMAS	−148.2	−163.5	−152.3	−154.4	
9	CDCl$_3$	−142.7 (ddqd)	−161.3 (dd)	−154.0 (ddd)	−158.3 (dd)	−62.7 (d)
		$^3J_{F5}$ = 19.3	$^3J_{F4}$ = 19.3	$^3J_{F5}$ = 19.3	$^3J_{F4}$ = 19.3	$^5J_{F4}$ = 12.9
		$^4J_{F6}$ = 3.0	$^3J_{F6}$ = 19.3	$^3J_{F7}$ = 19.3	$^3J_{F6}$ = 19.3	
		$^5J_{F7}$ = 19.3		$^4J_{F4}$ = 3.0		
		$^5J_{CF3}$ = 12.9				
	CPMAS	−141.2	−160.5	−154.5	−156.7	−63.0
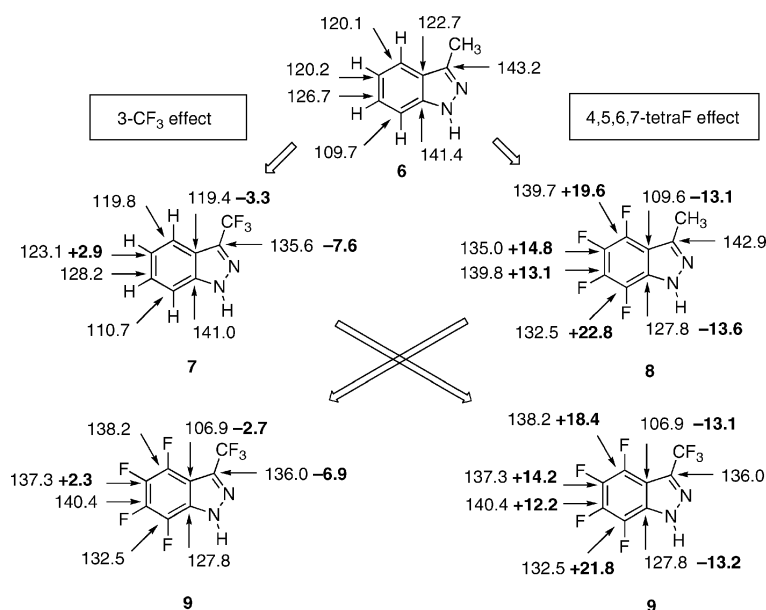
Scheme 5 Fluorine SCS on the ^{13}C signals for indazoles **6–9**.

although they are closer to the values of the helices than to those of the dimer. However, the values for the aromatic carbons and N-2 nitrogens clearly indicate that the needles of compound **8** should also be helical catemers.

Computational studies

How can we describe the difference in solid-state structure for dimer **6** and for helices **7** and **9**? It is reasonable to assume that the formation of indazole crystals of monomers **6–9** proceeds sequentially (Scheme 6). First, two molecules link together by one N–H···N hydrogen bond then they either form a dimer or a third molecule is linked and a catemer is formed.

In an attempt to determine the preferences for these two pathways we calculated at the B3LYP/6-31G* level the stabilization energies of the four possible dimers (dimer = two monomers). They are almost identical, 6_2 −53.8, 7_2 −52.5, 8_2 −54.6 and 9_2 −53.8 kJ mol^{-1}, and are unrelated to the formation of dimers, **6**, or catemers **7** and **9**. We can imagine that the difference could start from structure **16**, assuming that planar ones would lead to dimers and non-planar ones to catemers. However, the difference between the most stable planar and perpendicular arrangements is 21.5 kJ mol^{-1} for **16-6** and 22.3 kJ mol^{-1} for **16-7**, which obviously does not explain the observed structures. We have not been able to explain the secondary structure of indazoles, a problem that
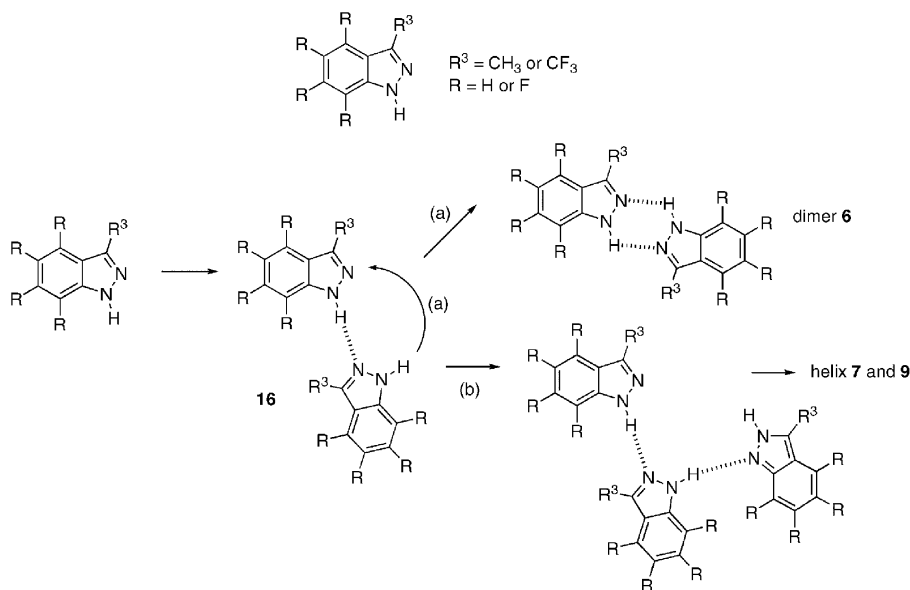
Scheme 6 Proposed sequence of events in the formation of indazole crystals.

This journal is © the Royal Society of Chemistry and the Centre National de la Recherche Scientifique 2007

Table 6 Differences (ppm) and ratios between the solution and the solid state chemical shifts

			Dimer 6	Helices 7 and 9	Indazole 8
^{13}C	R-3	Difference	1.5	1.15	0.9
		Ratio	1.143	1.010	1.074
^{13}C	Aromatic C	Difference	−1.0	1.5	1.3
		Ratio	0.992	1.011	1.010
^{15}N	N-1	Difference	2.8	−3.55	—[a]
		Ratio	0.986	1.018	—[a]
^{15}N	N-2	Difference	9.4	4.7	4.8
		Ratio	0.883	0.943	0.942

[a] Missing value of N-1 in compound 8 (Table 4).

must still be considered open. Note that in the case of the related pyrazoles there exists compounds like 3(5)-phenylpyrazole that crystallize in different motifs, tetramers, hexamers and catemers (polymorphism and desmotropy),[40] which means that the different pathways are very similar in energy. The observation that in a given crystal all the helices have the same parity (all of them *M* or all of them *P*) and in another crystal the situation could be the same or the reverse, *i.e.* each single crystal is enantiomerically pure, in opposition to all single crystals containing both *M* and *P* helices (racemic), is a problem related to crystal packing calculations.[41] Calculations aimed at determining the relative stability of both situations are outside the scope of the present paper and, for this reason, we can propose that indazole 8 would crystallize forming catemers, but there is no way to tell if the resulting crystals would be racemic or enantiomers.

Conclusion

For the first time, 3-methylindazole derivatives with different degrees of fluorination are observed to crystallize as helices with three-fold symmetry when fluorination is realized at either or both the benzo ring or the methyl group. This is demonstrated unequivocally by X-ray crystallography for compounds 7 and 9 and deduced from insightful NMR and computational studies for 8. 3-Methylindazole (6) forms discrete dimers. Providing a full rationale of the supramolecular arrangements is beyond the scope of this study; however, the helical supramolecular arrangement is proposed to be the result of strong N–H⋯N hydrogen bonds and aromatic interactions, both influenced by the presence of fluorine atoms. Compounds 7 and 9 are remarkable cases of non-chiral molecules that crystallize in chiral space groups.

Experimental

Compounds 3-methyl-1*H*-indazole 6 and 3-methyl-4,5,6,7-tetrafluoro-1*H*-indazole 8 were prepared according to published procedures.[16,19]

Synthesis of 3-trifluoromethyl-1*H*-indazole (7)

2-(2,2,2-Trifluoroacetyl)cyclohexanone (11). Cyclohexanone (10) (4 g, 40 mmol) was added to a mixture of sodium hydride (1.2 g, 50 mmol) and dry tetrahydrofuran (30 mL) contained in a 100 mL three-necked round bottom flask provided with a reflux condenser protected by a calcium chloride drying tube, and maintained under argon. The mixture was stirred and

Table 7 Crystal data and structure refinement

Compound	6	7	9
Formula	$C_8H_8N_2$	$C_8H_5F_3N_2$	$C_8HF_7N_2$
Formula weight	132.16	186.14	258.11
Temperature/K	180	180	180
λ (MoKα)/Å	0.71073	0.71073	0.71073
Crystal system	Monoclinic	Trigonal	Trigonal
Space group	$P2_1/n$	$P3_2$	$P3_2$
a/Å	8.9070(9)	12.5397(18)	12.5382(18)
b/Å	5.6894(8)	12.5397(18)	12.5382(18)
c/Å	13.0599(13)	4.3463(9)	4.9499(10)
β/°	90.588(12)	—	—
V/Å^3	661.78(13)	591.87(17)	673.90(19)
Z	4	3	3
ρ_{calcd}/Mg m^{-3}	1.327	1.567	1.908
μ/mm^{-1}	0.082	0.146	0.219
$F(000)$	280	282	378
Crystal size/mm	0.15 × 0.15 × 0.07	0.5 × 0.05 × 0.05	0.35 × 0.15 × 0.1
θ range/°	3.91–26.03	3.25–32.13	3.25–32.14
Index ranges	−10 ≤ h ≤ 10, −7 ≤ k ≤ 7, −16 ≤ l ≤ 15	−18 ≤ h ≤ 17, −17 ≤ h ≤ 18, −6 ≤ l ≤ 6	−18 ≤ h ≤ 18, −17 ≤ k ≤ 18, −7 ≤ l ≤ 6
Reflections collected/unique	4874/1224 R(int) = 0.0244	6295/1329 R(int) = 0.1597	7260/1520 R(int) = 0.0828
Completeness to θ/°	26.03 (94.7%)	32.13 (96.0%)	32.14 (95.9%)
Absorption corrections	Empirical (DIFABS)	Empirical (DIFABS)	Empirical (DIFABS)
Max/min transmission	0.992/0.989	0.991/0.931	0.974/0.928
Refinement method	Full-matrix least-squares on F^2	Full-matrix least-squares on F^2	Full-matrix least-squares on F^2
Data/restraints/parameters	1224/0/92	1329/1/118	1520/1/154
Goodness-of-fit on F^2	1.063	1.048	0.920
Final R indices $I > 2\sigma(I)$	R1 = 0.0368, wR2 = 0.0910	R1 = 0.0885, wR2 = 0.1489	R1 = 0.0418, wR2 = 0.071
R indices (all data)	R1 = 0.0420, wR2 = 0.0943	R1 = 0.1277, wR2 = 0.1687	R1 = 0.1385, wR2 = 0.0936
Largest diff. peak/hole/Å^3	0.185/−0.225	0.255/−0.246	0.177/−0.206

heated to reflux for 1 h (until the emission of gas ceased) and, after cooling, ethyl trifluoroacetate (7 g, 50 mmol) was added dropwise over a period of 2 h. The mixture was stirred at room temperature for 16 h. Isopropanol (3 mL) and water (40 mL) were then added and the mixture extracted with ether (3 × 50 mL) to remove undesired by-products (this portion was discarded). Concentrated hydrochloric acid was added to the remaining aqueous solution until pH 1 was reached. A brown oil formed which was extracted with ether (3 × 25 mL). After evaporation of the dried ethereal extracts, a dark oil (3.7 g) was obtained (48%), and used without further purification.

3-Trifluoromethyl-4,5,6,7-tetrahydro-1*H*-indazole (12). The crude product of 2-(2,2,2-trifluoroacetyl)cyclohexanone (**11**) (3.7 g, 19 mmol) was dissolved in ethanol (150 mL) in a round-bottomed flask equipped with a reflux condenser. Hydrazine monohydrate (1 g, 20 mmol) was added dropwise and the mixture was stirred and heated to reflux for 12 h. The mixture was cooled and the solvent removed *in vacuo*. The resulting dark viscous liquid was extracted with hexane (6 × 10 mL). The organic phase was evaporated yielding the desired product (2.3 g, 63%).

3-Trifluoromethyl-1*H*-indazole (7). 3-Trifluoromethyl-4,5,6,7-tetrahydro-1*H*-indazole (**12**) (0.5 g, 2.6 mmol), 0.22 g of palladium over carbon (10%) and anhydrous decalin (20 mL) were mixed in a three-necked flask equipped with a reflux condenser protected by a calcium chloride drying tube, and purged with argon. The reaction mixture was heated under reflux over 7 days. The solution was filtered warm and passed through a silica gel chromatography column (ether–hexane 1 : 5). Compound **7** (0.12 g, 25%) was obtained as a white solid after removing the volatiles. Mp: 95–97 °C (microscope). Mp 94–97 °C.[18] Elemental analysis (%) calcd for $C_8H_5F_3N_2$: C 51.62, H 2.71, N 15.05; found: C 51.55, H 2.93, N 14.84.

Synthesis of 3-trifluoromethyl-4,5,6,7-tetrafluoro-1*H*-indazole (9)

Octafluoroacetophenone (15)[42,43]. Pentafluorobromobenzene (**13**, 7.48 mL, 60 mmol) was dissolved in diethyl ether (50 mL) and cooled to −78 °C. *n*-Butyllithium (37.5 mL, 60 mmol), precooled to –78 °C, was added dropwise over a period of 30 min. The mixture was stirred for another 30 min at low temperature. After that time, a solution of methyl trifluoroacetate (5.99 mL, 60 mmol) in diethyl ether (35 mL) was quickly added at one time, and the reaction was stirred for 10 min, before being quenched with HCl (2 N, 150 mL) precooled to 0 °C. The two phases were separated at low temperature and the aqueous phase was extracted with diethyl ether (3 × 15 mL). The combined organic phases were dried over $MgSO_4$ and all volatiles were removed under slightly reduced pressure to yield a viscous brown-yellow liquid. This product was used without further purification. ^{19}F-NMR: (188.3 MHz, $CDCl_3$) δ (ppm) = −1.94 (t, J = 8.3, 3F, CF_3); −61.95 (m, 2F, $F_{arom.}$); −68.85 (m, 1F, $F_{arom.(para)}$); −83.30 (m, 2F, $F_{arom.}$).

3-Trifluoromethyl-4,5,6,7-tetrafluoro-1*H*-indazole (9). The reaction mixture of compound **15** was dissolved in toluene (50 mL) and cooled down to 0 °C. Hydrazine monohydrate (2.97 mL, 60 mmol) was then added dropwise and the mixture was stirred for another 2 h at low temperature. The reaction

mixture was then heated to reflux for 16 h, yielding a yellow mixture with a brown aqueous phase. The phases were separated and the aqueous phase was extracted with toluene (3 × 5 mL). The combined organic phases were dried over $MgSO_4$ and all volatiles were removed *in vacuo*, yielding a red-brown viscous liquid, which was purified by column chromatography (CH_2Cl_2–pentane 3 : 1). The resulting white solid was usually polluted by an orange oil. Recrystallization from pentane yielded 4.95 g of the desired product (19 mmol, total yield from pentafluorobromobenzene, 32%) as a white solid. Mp 70–71 °C. Using pure **15** (1 g, 3.8 mmol) as the staring material, a yellow oil (0.77 g, 79% yield) was obtained. Crystallization from hexane yielded **9**. Mp: 71–73° C (microscope). Elemental analysis (%) calcd for $C_8HF_7N_2$: C 37.23, H 0.39, N 10.85; found: C 37.13, H 0.52, N 10.68.

X-Ray crystallography

Two structures (compounds **7** and **9**) were recorded at low temperature (180 K) on an Xcalibur Oxford Diffraction diffractometer equipped with an Oxford Cryosystems Cryostream Cooler Device using a graphite-monochromated Mo-Kα radiation (λ = 0.71073 Å). The structure of compound **6** was recorded at low temperature (180 K) on an IPDS STOE diffractometer equipped with an Oxford Cryosystems Cryostream Cooler Device using a graphite-monochromated Mo-Kα radiation (λ = 0.71073 Å). Data collection, data reduction and refinement of the structures proceeded smoothly. Table 7 contains a summary of crystal and refinement data. Details can be found in the electronic supplementary information (ESI).†

Compounds **7** and **9** crystallized in a chiral group. Since there were no significant anomalous scatterers, there was no way to choose between the space groups $P3_1$ and $P3_2$. $P3_2$ was arbitrarily chosen. Similarly, we were not able to determine their absolute configuration. Indeed, there is no possibility to refine the Flack parameter since the structures do not contain any atoms heavier than Si, and the measurements have been recorded using Mo radiation. Drawing of molecules (Fig. 1, 3 and 4) was performed with the program ORTEP32[44] with 30% probability displacement ellipsoids for non-hydrogen atoms. Fig. 2 and 5–9 were obtained with the software Mercury.[45]

CCDC 615981 (**6**), CCDC 615982 (**7**), and CCDC 615983 (**9**), contain the supplementary crystallographic data for this paper.‡

NMR spectroscopy

Solution spectra devices and procedures were routine. Details can be found in the ESI.†

Solid state [13]C (100.73 MHz) and [15]N (40.60 MHz) CPMAS NMR spectra have been obtained on a Bruker WB 400 spectrometer at 300 K using a 4 mm DVT probe head. Samples were carefully packed in a 4 mm diameter cylindrical zirconia rotors with Kel-F end-caps. Operating conditions involved 3.2 μs 90° [1]H pulses and decoupling field strength of 78.1 kHz by TPPM sequence. [13]C spectra were originally referenced to a glycine sample and then the chemical shifts were recalculated to Me_4Si (for the carbonyl atom δ(glycine)

= 176.1 ppm) and ^{15}N spectra, to ^{15}NH$_4$Cl and then converted to the nitromethane scale using the relationship: δ^{15}N(nitromethane) = δ^{15}N(ammonium chloride) = 338.1 ppm. The typical acquisition parameters for ^{13}C CPMAS were: spectral width, 40 kHz; recycle delay, 5 s; acquisition time, 30 ms; contact time, 2 ms; and spin rate, 12 kHz. In order to distinguish protonated and unprotonated carbon atoms, the NQS (non-quaternary suppression) experiment by conventional cross-polarization was recorded; before the acquisition the decoupler is switched off for a very short time of 25 μs. The typical acquisition parameters for ^{15}N CPMAS were: spectral width, 40 kHz; recycle delay, 5 s; acquisition time, 35 ms; contact time, 6 ms; and spin rate, 6 kHz. ^{19}F (376.01 MHz) CPMAS NMR spectra have been obtained with a Bruker WB 400 spectrometer at 300 K using a 2.5 mm DVT probe head. Samples were carefully packed in a 2.5 mm diameter cylindrical zirconia rotors with Kel-F end-caps. The spectra were referenced to CFCl$_3$. The typical acquisition parameters for ^{19}F CPMAS were: spectral width, 100 kHz; recycle delay, 10 s; acquisition time, 20 ms; contact time, 5 ms; and spin rate, 30 kHz.

GIAO calculations

Geometries of compounds **6–9** were fully optimized at the B3LYP theoretical level,[46,47] with the 6-31G* basis[48] and the 6-311+ +G** basis sets,[49] as implemented in the Gaussian 03 program.[50] Harmonic frequency calculations[51] verified the nature of the stationary points as minima (all real frequencies). Absolute shieldings of compounds **1–6** have been calculated over the fully optimized geometries within the GIAO approximation.[52] The differences in energy between 1H and 2H tautomers as well as the GIAO absolute shieldings were calculated at the B3LYP/6-311+ +G** level, while the energies of the dimers was calculated at the B3LYP/6-31G* level.

Acknowledgements

References

1 (a) J. Elguero, P. Goya, N. Jagerovic and A. M. S. Silva, Pyrazoles as Drugs: Facts and Fantasies, in *Targets in Heterocyclic Systems*, ed. O. A. Attanasi and D. Spinelli, Italian Society of Chemistry, Roma, 2002, vol. 6, p. 69; (b) J. Elguero, P. Goya, N. Jagerovic and A. M. S. Silva, Pyrazoles as Drugs: Facts and Fantasies, in *Targets in Heterocyclic Systems*, ed. O. A. Attanasi and D. Spinelli, Italian Society of Chemistry, Roma, 2002, vol. 6, p. 72.

2 S. Hegde and M. Schmidt, Too Market, To Market—2004, *Annu. Rep. Med. Chem.*, 2005, **40**, 459.

3 (a) R. C. Babbedge, P. A. Bland-Ward, S. L. Hart and P. K. Moore, *Br. J. Pharmacol.*, 1993, **110**, 225–228; (b) P. K. Moore and P. A. Bland-Ward, *Methods Enzymol.*, 1996, **268**, 393–399; (c) P. Schumann, V. Collot, Y. Hommet, W. Gsell, F. Dauphin, J.

Sopková, E. MacKenzie, D. Duval, M. Boulouard and S. Rault, *Bioorg. Med. Chem. Lett.*, 2001, **11**, 1153–1156; (d) J. Sopková-de Oliveira Santos, V. Collot and S. Rault, *Acta Crystallogr., Sect. C: Cryst. Struct. Commun.*, 2002, **C58**, o688–o690.

4 J. A. Olsen, D. W. Banner, P. Seiler, U. Obst Sander, A. D'Arcy, M. Stihle, K. Müller and F. Diederich, *Angew. Chem., Int. Ed.*, 2003, **42**, 2507–2511.

5 (a) Editorial:, Unveiling the Mystery and Beauty of Organic Fluorine, *ChemBioChem*, 2004, **5**, 559–562; (b) J. D. Dunitz, *ChemBioChem*, 2004, **5**, 614–621; (c) A. M. Thayer, Fabulous Fluorine, *Chem. Eng. News*, 2006, **84**, 15–24.

6 K. Reichenbächer, H. I. Süss and J. Hulliger, *Chem. Soc. Rev.*, 2005, **34**, 22–30.

7 (a) W. Peti, T. Pieper, M. Sommer, B. K. Keppler and G. Giesler, *Eur. J. Inorg. Chem.*, 1999, 1551–1555; (b) A. Carella, J. Jaud, G. Rapenne and J.-P. Launay, *Chem. Commun.*, 2003, 2434–2435; (c) A. Egger, V. B. Arion, E. Reisner, B. Cebrián-Losantos, S. Shova, G. Trettenhahn and B. K. Keppler, *Inorg. Chem.*, 2005, **44**, 122–132; (d) P. Oulié, J. Teichert, L. Vendier, C. Dablemont and M. Etienne, *New J. Chem.*, 2006, **30**, 679–682.

8 J. Elguero, C. Marzin, A. R. Katritzky and P. Linda, *The Tautomerism of Heterocycles*, Academic Press, New York, 1976.

9 J. Catalán, J. L. G. de Paz and J. Elguero, *J. Chem. Soc., Perkin Trans. 2*, 1996, 57–60.

10 I. Alkorta and J. Elguero, *J. Phys. Org. Chem.*, 2005, **18**, 719–724.

11 J. Elguero, A. Fruchier and R. Jacquier, *Bull. Soc. Chim. Fr.*, 1966, 2075–2084.

12 J. Elguero, A. Fruchier, E. M. Tijou and S. Trofimenko, *Chem. Heterocycl. Compd.*, 1995, **31**, 1006–1026.

13 R. M. Claramunt, D. Sanz, C. López, J. A. Jiménez, M. L. Jimeno, J. Elguero and A. Fruchier, *Magn. Reson. Chem.*, 1997, **35**, 35–75.

14 C. Foces-Foces, *Acta Crystallogr., Sect. E: Struct. Rep. Online*, 2005, **E61**, o337–o339.

15 L. C. Behr, Indazoles and Condensed Types, , in *Pyrazoles, Pyrazolines, Pyrazolidines, Indazoles and Condensed Rings*, ed. R. H. Wiley, Interscience, New York, 1967, p. 319.

16 R. Huisgen and K. Bast, *Org. Synth.*, 1962, **42**, 69–71.

17 V. Dupré, J. Pechmeze and R. Sureau, *Ger. Offen.*, 2 513 801, 02 Oct 1975 (*Chem. Abs.*, 1976, **84**, 17337x).

18 D. K. O'Dell and K. M. Nicholas, *Heterocycles*, 2004, **63**, 373–382.

19 B. A. Hathaway, G. Day, M. Lewis and R. Glaser, *J. Chem. Soc., Perkin Trans. 2*, 1998, 2713–2719.

20 C. A. Hunter, K. R. Lawson, J. Perkins and C. J. Urch, *J. Chem. Soc., Perkin Trans. 2*, 2001, 651–669.

21 M. Nishio, *CrystEngComm*, 2004, **6**, 130–158.

22 (a) I. Alkorta, I. Rozas and J. Elguero, *J. Org. Chem.*, 1997, **62**, 4687–4691; (b) I. Alkorta, I. Rozas and J. Elguero, *J. Am. Chem. Soc.*, 2002, **124**, 8593–8598; (c) C. Garau, A. Frontera, D. Quiñonero, P. Ballester, A. Costa and P. M. Deyà, *Chem. Phys. Lett.*, 2004, **392**, 85–89.

23 (a) J. Elguero, A. Fruchier, N. Jagerovic and A. Werner, *Org. Prep. Proced. Int.*, 1995, **27**, 33–74; (b) M. A. P. Martins, N. Zanatta, H. G. Bonacorso, F. A. Rosa, R. M. Claramunt, M. A. García, M. D. Santa María and J. Elguero, *ARKIVOC*, 2006iv), 29–37; (c) R. M. Claramunt, P. Cornago, V. Torres, E. Pinilla, M. R. Torres, A. Samat, V. Lokshin, M. Valés and J. Elguero, *J. Org. Chem.*, 2006, **71**, 6881–6891.

24 C. Foces-Foces, F. H. Cano and J. Elguero, *Gazz. Chim. Ital.*, 1993, **123**, 477–479.

25 C. Foces-Foces, I. Alkorta and J. Elguero, *Acta Crystallogr., Sect. B: Struct. Sci.*, 2000, **B56**, 1018–1028.

26 A. Gzella, U. Wrzeciono, J. Dudzinska-Usarewicz and T. Borowiak, *Acta Crystallogr., Sect. C: Cryst. Struct. Commun.*, 1989, **C45**, 642–644.

27 (a) J. Sopková-de Oliveira Santos, V. Collot and S. Rault, *Acta Crystallogr., Sect. C: Cryst. Struct. Commun.*, 2000, **C56**, 1503–1504; (b) F. Ooms, B. Norberg, E. M. Isin, N. Castagnoli, C. J. Van der Schyf and J. Wouters, *Acta Crystallogr., Sect. C: Cryst. Struct. Commun.*, 2000, **C56**, e474–e475.

28 A. Gzella and U. Wrzeciono, *Acta Crystallogr., Sect. C: Cryst. Struct. Commun.*, 2001, **C57**, 1189–1191.

29 O. Hager, C. Foces-Foces, N. Jagerovic, J. Elguero and S. Trofimenko, *Acta Crystallogr., Sect. C: Cryst. Struct. Commun.*, 1996, **C52**, 2894–2896.

30 M. A. García, C. López, R. M. Claramunt, A. Kenz, M. Pierrot and J. Elguero, *Helv. Chim. Acta*, 2002, **85**, 2763–2776.
31 A. A. Dvorkin, A. S. Javorskii, Y. A. Simonov, G. E. Golodeev, S. A. Andronati and T. I. Malinovskii, *Dokl. Akad. Nauk SSSR*, 1989, **305**, 1378–1382.
32 R. Glaser, C. L. Mummert, C. J. Horan and C. L. Barnes, *J. Phys. Org. Chem.*, 1993, **6**, 201–214.
33 A. Escande and J. Lapasset, *Acta Crystallogr., Sect. B: Struct. Crystallogr. Cryst. Chem.*, 1974, **B30**, 2009–2012.
34 J. Jacques, A. Collet and S. H. Willen, *Enantiomers, Racemates, and Resolutions*, Krieger Publishing Company, Malabar, Florida, 1994.
35 R. Perrin, R. Lamartine, M. Perrin and A. Thozet, Solid state chemistry of phenols and possible industrial applications, , in *Organic Solid State Chemistry*, ed. G. R. Desiraju, Elsevier, Amsterdam, 1987, ch. 8, p. 284.
36 J. Catalán, F. Fabero, M. S. Guijarro, R. M. Claramunt, M. D. Santa María, M. C. Foces-Foces, F. H. Cano, J. Elguero and R. Sastre, *J. Am. Chem. Soc.*, 1990, **112**, 747–759.
37 S. Berger, S. Braun and H.-O. Kalinowski, *NMR Spectroscopy of the Non-Metallic Elements*, John Wiley and Sons, Chichester, 1997, pp. 450–451.
38 I. Alkorta and J. Elguero, *Struct. Chem.*, 1998, **9**, 187–202.
39 J. R. Yates, T. N. Pham, C. J. Pickard, F. Mauri, A. M. Amado, A. M. Gil and S. P. Brown, *J. Am. Chem. Soc.*, 2005, **127**, 10216–10220.
40 I. Alkorta, J. Elguero, C. Foces-Foces and L. Infantes, *ARKIVOC*, 2006ii), 15–30.
41 (*a*) R. Boese, M. T. Kirchner, J. D. Dunitz, G. Filippini and A. Gavezzotti, *Helv. Chim. Acta*, 2001, **84**, 1561–1577; (*b*) J. D. Dunitz, *Chem. Commun.*, 2003, 545–548; (*c*) A. Gavezzotti, *CrystEngComm*, 2003, **5**, 429–438; (*d*) A. Gavezzotti, *CrystEngComm*, 2003, **5**, 439–446.
42 K.-R. Pörschke and D. Alberti, *Organometallics*, 2004, **23**, 1459–1460.
43 L. S. Chen, G. J. Chen and C. Tamborski, *J. Fluorine Chem.*, 1981, **18**, 117–129.
44 ORTEP3 for Windows: L. J. Farrugia, *J. Appl. Crystallogr.*, 1997, **30**, 565.
45 I. J. Bruno, J. C. Cole, P. R. Edgington, M. K. Kessler, C. F. Macrae, P. McCabe, J. Pearson and R. Taylor, *Acta Crystallogr., Sect. B: Struct. Sci.*, 2002, **B58**, 389–397.
46 R. G. Parr and W. Yang, *Density-Functional Theory of Atoms and Molecules*, Oxford, New York, 1989.
47 L. J. Bartolotti and K. Fluchick, in *Reviews in Computational Chemistry*, ed. K. B. Lipkowitz and D. B. Boyd, VCH Publishers, New York, 1996, vol. 7, pp. 187–216.
48 P. A. Hariharan and J. A. Pople, *Theor. Chim. Acta*, 1973, **28**, 213–222.
49 M. J. Frisch, J. A. Pople, R. Krishnam and J. S. Binkley, *J. Chem. Phys.*, 1984, **80**, 3265–3269.
50 M. J. Frisch, G. W. Trucks, H. B. Schlegel, G. E. Scuseria, M. A. Robb, J. R. Cheeseman, J. A. Montgomery, Jr., T. Vreven, K. N. Kudin, J. C. Burant, J. M. Millam, S. S. Iyengar, J. Tomasi, V. Barone, B. Mennucci, M. Cossi, G. Scalmani, N. Rega, G. A. Petersson, H. Nakatsuji, M. Hada, M. Ehara, K. Toyota, R. Fukuda, J. Hasegawa, M. Ishida, T. Nakajima, Y. Honda, O. Kitao, H. Nakai, M. Klene, X. Li, J. E. Knox, H. P. Hratchian, J. B. Cross, V. Bakken, C. Adamo, J. Jaramillo, R. Gomperts, R. E. Stratmann, O. Yazyev, A. J. Austin, R. Cammi, C. Pomelli, J. Ochterski, P. Y. Ayala, K. Morokuma, G. A. Voth, P. Salvador, J. J. Dannenberg, V. G. Zakrzewski, S. Dapprich, A. D. Daniels, M. C. Strain, O. Farkas, D. K. Malick, A. D. Rabuck, K. Raghavachari, J. B. Foresman, J. V. Ortiz, Q. Cui, A. G. Baboul, S. Clifford, J. Cioslowski, B. B. Stefanov, G. Liu, A. Liashenko, P. Piskorz, I. Komaromi, R. L. Martin, D. J. Fox, T. Keith, M. A. Al-Laham, C. Y. Peng, A. Nanayakkara, M. Challacombe, P. M. W. Gill, B. G. Johnson, W. Chen, M. W. Wong, C. Gonzalez and J. A. Pople, *GAUSSIAN 03*, Gaussian, Inc., Wallingford, CT, 2004.
51 J. W. McIver and A. K. Komornicki, *J. Am. Chem. Soc.*, 1972, **94**, 2625–2633.
52 (*a*) R. Ditchfield, *Mol. Phys.*, 1974, **27**, 789–807; (*b*) F. London, *J. Phys. Radium*, 1937, **8**, 397–409.

This journal is © the Royal Society of Chemistry and the Centre National de la Recherche Scientifique 2007